Basin Research

IAS EAGE

Basin Research (2012) **24**, 338–356, doi: 10.1111/j.1365-2117.2011.00526.x

Analysis of the Devonian (Frasnian) platform from Belgium: a multi-faceted approach for basin evolution reconstruction

Anne-Christine Da Silva and Frédéric Boulvain

Department of Geology, University of Liège, Liège, Belgium

ABSTRACT

This study undertakes a multi-disciplinary approach (sedimentology, carbon isotopes, magnetic susceptibility and thickness distribution) to improve understanding of a major Palaeozoic carbonate platform, the Frasnian platform of Belgium. These combined techniques are used to reconstruct the platform history, which evolved in two main steps. During the first phase, the basin was strongly influenced by faulting, producing notable thickness and facies variations, with open ocean conditions, with good water circulation and no/or limited barrier reef. The second phase of platform development was less influenced by differential subsidence, as indicated by homogeneous facies distribution. However, this platform developed under restricted waters, with low circulation which is likely related to the development of a barrier reef.

INTRODUCTION

Ancient carbonate platforms are sometimes difficult to understand because the platforms are often incomplete (due to tectonic deformation and diagenesis) and as the environmental conditions and the faunas were different, actualism is not always the appropriate answer. The Belgian Frasnian platform was affected by the Variscan Orogeny, leading to the formation of a fold and thrust belt and to the loss of the major part of the platform. For example, debates remain about the existence of a barrier reef system in Belgium during the Frasnian. Tsien (1984) interpreted the Merlemont dolomite outcrop in the Philippeville Anticlinorium as a barrier reef but Boulvain *et al.* (1994) interpreted it as a restricted lagoonal deposit formed in the centre of an atoll.

This study undertakes a multi-faceted approach to provide a comprehensive interpretation of the Belgian Frasnian platform. It brings together many data sets and applies several analytical techniques, to stratigraphic sections from a variety of platforms. Detailed sedimentological analysis investigates the depositional palaeoenvironments and their evolution through time and space. Magnetic susceptibility (MS) aids identification of sea-level changes, stratigraphic correlations and highlights the influence of detrital input (Da Silva & Boulvain, 2006). Carbon isotope geochemistry provides insight into complex interactions between production of organic matter and water circulation on a platform (Da Silva & Boulvain, 2008). Furthermore, this article uses variations in sediment thickness to reconstruct platform geometry and interpret differential subsidence. This integrated approach is used to better constrain the timing and relationships between sea-level changes, water circulation, sediment supply and platform geometry.

Correspondence: Anne-Christine Da Silva, Department of Geology, University of Liège, Sedimentary Petrology, B20, 4000 Liège, Belgium. E-mail: ac.dasilva@ulg.ac.be

GEOLOGICAL SETTING

Southern Belgium has well exposed Palaeozoic limestones that are historical stratotypes for several stages of the Devonian (d'Omalius d'Halloy, 1862). This setting provides a good opportunity to apply various techniques across carbonate depositional environments within a well developed palaeontological and stratigraphic framework. During the Frasnian, southern Belgium (relicts of Devonian basins contained in the Variscan allochton) was located between the Southern Tropic and the palaeoequator. The main landmasses (and detrital sources) were located to the north (Brabant Massif) and depositional environments generally deepen towards the south east. During the Devonian, southern Belgium was located on the southern border of Laurussia, the so-called 'Old Red Continent'; which was a passive extensional margin affected by syn-sedimentary faults (Floyd, 1982; Von Winterfeld, 1994; Adams & Vandenberghe, 1999; Oncken *et al.*, 1999; Franke, 2000; Lacquement & Meilliez, 2006; Salamon & Königshof, 2010). Syn-sedimentary NE- and WNW-striking faults subdivided the Rhenohercynian passive margin (platforms and their slopes) during the Early Devonian to Mississippian (e.g. Meilliez & Mansy, 1990; Fielitz, 1992, 1997). These syn-sedimentary faults are commonly identified through marked lateral thickness and facies variations. The location of these synsedimentary extensional faulting was proposed for the Givetian

(Kasimi & Preat, 1996) and for the Famennian (Paproth *et al.*, 1986) Belgian platforms, but was still missing for the Frasnian platform. These structures had a major influence on the subsequent formation of the Rhenohercynian fold and thrust belt as they delimitated domains of different rheology and competence which were characterized by different internal deformation. During the Variscan Orogeny, basin closure (Franke, 2000) led to the inversion of main synsedimentary faults (Fielitz, 1992; Vanbrabant *et al.*, 2002).

This study concerns mainly the Frasnian, from *punctata* to the lower part of Lower *rhenana* conodont zones (Gouwy & Bultynck, 2000) and during this time, different formations, corresponding to major palaeoenvironments are observed, from the south to the north (Figs 1 and 2; Boulvain *et al.*, 1999):

- Southern Area (SA) – southern border of the Dinant Synclinorium: most distal part of the platform; this area presents a succession of three carbonate mounds separated by argillaceous intervals (Arche and La Boverie mounds in the Moulin Liénaux Formation and Lion mound in the Grands Breux Formation).
- Central Philippeville Area (CPh) – Philippeville Anticlinorium: argillaceous and nodular crinoidal marls and lenses of stromatoporoid-coral coverstones during the Pont de la Folle Formation and dark crinoidal argillaceous carbonates overlain by biostromal and shallow-water facies of the Philippeville Formation.

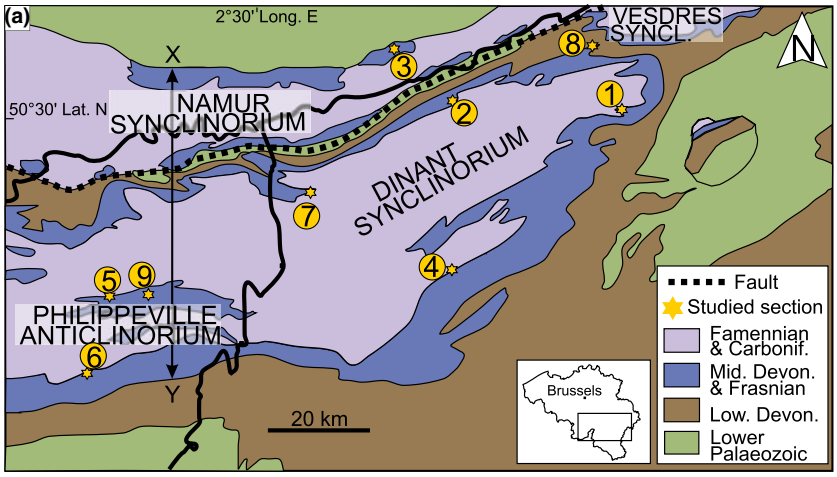

n° Section	Formations	Location	Thick.	Sples
1. Aywaille	Lustin	EDS	120 m	261
2. Barse	Lustin	NDS	46 m	120
3. Huccorgne	Bovesse - Huccorgne	NNS	165 m	213
4. La Boverie	Moulin Liénaux-Grands Breux	SDS	168 m	260
5. Neuville	Philippeville	PA	70 m	160
6. Nord	Moulin Liénaux -Grands Breux	SDS	159 m	190
7. Tailfer	Lustin	NDS	105 m	268
8. Tilff	Lustin	EDS	90 m	136
9. Villers	Philippeville	PA	105 m	242

Fig. 1. Geological setting of the Frasnian in Belgium. (a) Geological map of southern Belgium, with location of studied sections, numbers are explained on (c); (b) north–south cross-section through the Belgian Frasnian sedimentary basin, before Variscan deformation and corresponding areas. Section numbers are explained on (c) and letters *X* and *Y* correspond to the cross-section line *X*–*Y* on (a); (c) table with numbers of the sections and corresponding section names, corresponding formation names, locations (EDS-NDS-SDS, East-North-South Dinant Synclinorium; NNS, North Namur Synclinorium; PA, Philippeville Anticlinorium), Thick., thickness; Sples, number of samples.

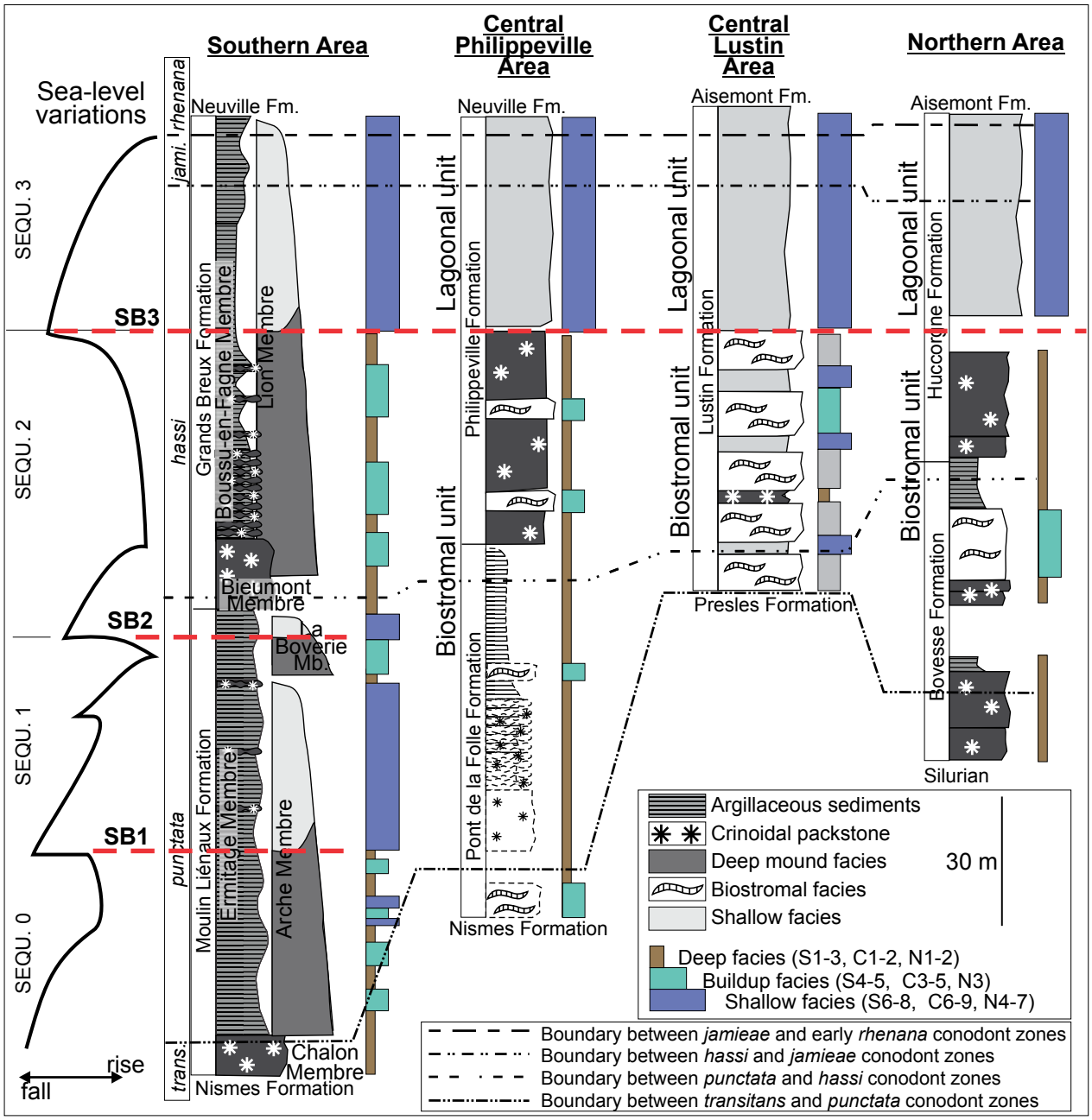

Fig. 2. Correlations from the different areas developed during the Frasnian Belgian platform, with facies evolution. Conodont zonations are from Gouwy & Bultynck (2000). Sea-level changes are from Da Silva *et al.* (2010). Pont-de-la-Folle Formation is in dotted line as most of the data are from literature (no continuous outcrops). Legend is on Fig. 3d.

- Central Lustin Area (CL) – northern and eastern borders of the Dinant Synclinorium, southern border of the Namur Synclinorium and Vesdres Synclinorium: the Lustin Formation is dominated by stromatoporoid biostromes and shallow-water facies.
- Northern Area (NA) – north eastern border of the Namur Synclinorium: this area is characterized by rare outcrops and there is no continuous Frasnian section. The Bovesse Formation corresponds to an alternation of dolomite with tabulate corals, shales, marls and dark limestones. The Huccorgne Formation is composed of dark thinly bedded limestones overlain by shallow-water facies. The contact between the two formations is a gap in the outcrop.

TECHNIQUES

In this study, microfacies analysis was undertaken on more than 1600 thin sections from nine outcrops (La Boverie and Nord quarries (Moulin Liénaux and Grands Breux Formations), Villers, Neuville (Philippeville Formation), Tailfer, Aywaille, Tilff and Barse (Lustin

Formation) and Huccorgne (Bovesse and Huccorgne formations). The interval between two samples is typically 50 cm, except in Nord quarry (1 m). Facies and microfacies were compared with classical models (Hardie, 1977; Flügel, 2004) and specifically with other Devonian platforms (Méndez-Bedia *et al.*, 1994; George *et al.*, 1997, 2009; Pohler, 1998; Whalen *et al.*, 2000; Chen *et al.*, 2001; Macneil & Jones, 2006).

Magnetic susceptibility is a measure of the response of a sample to an applied magnetic field. MS of a rock depends on its mineralogical composition, mineral grain size, shape of the mineral and orientation of the mineral grains (detailed method in Da Silva & Boulvain, 2006).

Carbon isotopic analyses were performed on carbonate matrix and the whole data set corresponds to 187 measurements, including 130 analyses from the Tailfer section (previously published in Da Silva & Boulvain, 2008), and the other data are provided for comparisons and insight into lateral variability in carbon isotopes from Huccorgne (9), Villers (11), Neuville (11) and La Boverie (26). Samples consisted of the finest grained carbonate mudstone, without luminescence, with a minimal quantity of skeletal grains, clays and calcite veins. The isotopic analyses were performed at the Institute of Geology and Mineralogy of the University of Erlangen (Germany) (see detailed method in Da Silva & Boulvain, 2008).

SEDIMENTOLOGY, FACIES AND CYCLICITY

As presented in the Geological setting, the Frasnian in Belgium is laterally and vertically subdivided in different formations, interpreted as recording different palaeoenvironmental settings (Figs 1 and 2). The SA (carbonate mounds) sedimentological model was described in Boulvain (2001, 2007) and Da Silva & Boulvain (2004). Facies in the CPh and CL are similar and therefore described by one model (Da Silva & Boulvain, 2004). The NA represents a third model not presented before. A synthesis of facies is presented in Table 1.

Depositional model for the Southern Area (SA)

The coding scheme used herein for designating the mud mound facies follows Boulvain (2007), in that identical facies are given identical facies numbers, even when they are present in mounds at different stratigraphic levels.

Off mound facies (S0-0b) are composed of argillaceous sediment (S0) and argillaceous crinoidal packstone (S0b). Both microfacies are interpreted as being deposited below the fair weather wave base (FWWB) but above storm wave zone (SWZ). Deep mound facies (S2–S5) correspond to muddy and peloidal facies with abundant stromatactis, crinoids and corals (S2) or stromatoporoids (S3), udoteacean algae and branching stromatoporoid floatstone (S4) and microbial facies (stromatolithes, trombolithes, clotted matrix) (S5). S3 developed close to the storm wave base in a subphotic environment, S4 is characterized by the occurrence of green algae and developed close to the fair weather wave base in a photic environment and S5 is observed as lenses in S3 or S4. Shallow mound inner facies (S6–S8) corresponds to branching and bulbous stromatoporoid rudstone (S6), peloidal laminated limestone (and/or loferites) (S7) and bioturbated mudstone (S8) and are all observed in the centre of the mounds and are interpreted as very shallow water.

Table 1. Microfacies from Southern, Central and Northern Areas with the main characteristics for each area underlined

	Southern Area	Central Area	Northern Area
Deep facies	S0: shales S0b: argillaceous crinoidal packstone	C1: shales with carbonated intercalations C2: crinoidal micropackstone to wackestone with ostracods and sponge spicules	N1: laminated or bioturbated shales N2: mudstone to packstone with gastropods and crinoids
Buildup facies	S2: mud, peloids with stromatactis, crinoids, corals S3: mud with stromatoporoids S4: udoteacean algae and branching stromatoporoids floatstone S5: microbial facies	C3: laminar stromatoporoids with high mud content C4: high domical stromatoporoid rudstone C5: branching stromatoporoid floatstone	N3: dolomitized biostrome with branching and massive stromatoporoid and branching tabulate corals.
Shallow facies	S6: *Amphipora* and high domical stromatoporoid S7: laminated peloidal grainstone S8: bioturbated mudstone	C6: *Amphipora* floatstone, peloids and algae C7: mudstone to wackestone with *Umbella* and ostracods C8: laminated peloidal grainstone C9: paleosols	N4: *Amphipora* floatstone, peloids and algae N5: algal packstone to boundstone, oncoids N6: mudstone to wackestone with *Umbella* and ostracods N7: laminar grainstone with peloids and clasts

Facies S1 was observed in the Upper Frasnian mounds but not in these outcrops, so facies S1 is not described herein (for description, refer to Boulvain, 2001).

Facies succession (Fig. 2) was described in detail in Boulvain (2007) and is based on the subdivision of all buildups in two main parts: a lower part dominated by deeper facies (S1–S5) and a second part dominated by shallower facies (S6–S8). The bases of the Lion and Arche mounds (Fig. 2) are characterized by off mound facies (S0), overlain by the deepest mound facies (S3–S5). After about 30–80 m of stacking of this facies forming the bulk of the mounds, reworking facies developed on the flank of the mound and restricted shallow-water facies developed in the central part of the buildups (S6–S8) (around 75 m of shallow-water facies). This geometry suggests the development of an area of restricted sedimentation, i.e. an inner shallow lagoon, sheltered by the bindstone or floatstone facies (S4) of the mound margin. The same geometry is observed in the Arche and Lion buildups (Fig. 1) and the name 'atoll-like mound' was suggested for these members (Boulvain *et al.*, 2004). The intermediate La Boverie mound is thinner than the two other mounds (Arche and Lion mounds are more than 100 m thick, La Boverie mound is around 50 m thick) and until now, no data are available on its geometry, but the evolution from deep to shallow facies is similar to what is observed in the other mounds. Development of the mounds is interpreted as closely related to sea-level changes (Boulvain, 2007): reef initiation occurred during transgression with development of the deepest facies and off mound deposits (S0–S5). Subsequent sea-level drop restricted reef growth to downslope locations and this is associated with emergence and synsedimentary lithification (Sandberg *et al.*, 1992), local development of pendant cement, karstic features (pictures in Da Silva *et al.*, 2010 in Fig. 5) and/or very sharp facies change (commonly S2 or S3 to S6 or S7). The following transgressive stage (S5–S6), led to the development of a circular reef margin (atoll 'corona'). Therefore, the occurrence of restricted shallow-water inner facies (S6–S8) inside this corona is possibly the result of a balance between sea-level rise and reef growth. As a result, sequence stratigraphic development is probably similar for the three mound levels (Fig. 2; Boulvain, 2007; Da Silva *et al.*, 2010). Sequence 0 is not complete (upper part of a transgressive system track (TST) and a high stand system track (HST)) and corresponds to the base of the Arche mound (deep facies), and is capped by the first sequence boundary (SB1), overlained by Sequence 1 (TST and HST), composed of the upper part of Arche mound (shallow facies), and lower part of the La Boverie mound (deep facies). The shallow part of the La Boverie mound and the lower deep part of the Lion mound correspond to Sequence 2, capped by SB3. Base of Sequence 3 corresponds to the upper part of the Lion mound (shallow-water facies) (Fig. 2).

Depositional model for the Central Area (CA)

The deep facies belt (C1–C2) consists of shales with some carbonate intercalations (C1 similar to S0 to S0b) and decimetre bedded crinoidal wackestone with possible sponge spicules and ostracods (C2), within a micropackstone matrix. Both microfacies are interpreted as being deposited below the FWWB but within the distal SWZ. These facies are mostly observed in the CPh, with only a minor distribution in the CL. The biostromal belt (C3–C5) is composed of biostromes mainly constructed by stromatoporoids with different morphologies: laminar stromatoporoid biostromes (C3), rudstone with high domical stromatoporoids and rugose and tabulate corals (C4) and floatstone composed of dendroid stromatoporoids (C5). These microfacies correspond to biostromes developed within variable wave energy, close to or within the FWWB. The shallow platform (C6–C9) presents a subtidal to supratidal succession. Subtidal facies (C6) are characterized by *Amphipora* floatstone, peloidal and palaeosiphonocladales packstone. Intertidal facies consist of *Umbella* (calcified part of charophytes) and ostracods wackestone or packstone (C7) and laminated grainstone with peloids (C8). The supratidal zone (C9) is characterized by brecciated decimetre- to metre-thick intervals with desiccation and circum-granular cracks and pendant cement corresponding to well develop paleosols.

In the CA, the sections are divided in two main units (Fig. 2), a lower unit characterized by deep and biostromal facies assemblages and an upper unit composed of shallow facies. The boundary between the two units is interpreted as a sequence boundary (Boulvain & Coen-Aubert, 1997; Da Silva *et al.*, 2009a) and is characterized by various features such as scalloped sharp surface with centimetre-scale relief, local red staining and centimetre-thick argillite unit. After Strasser & Hillgärtner (1998), in shallow water to supratidal environments, argillaceous levels could be related to sequence boundary (when associated to charophytes as observed here); through increasing erosion or through low-energy conditions and settling out of the clay).

Depositional model for the Northern Area (NA)

The deep belt (N1–N2) is composed of laminated or bioturbated shales with local concentration of pyrite and dolomite (N1 similar to S0 and C1), interpreted as deposited under the FWWB. Facies N2 is a crinoidal mudstone to packstone (Table 1), with gastropods. Locally, some bioclastic accumulations are observed with the same dominant organisms, and a few brachiopods, ostracods, bryozoans, trilobites and clasts, with some strongly altered paleosiphonocladales and *Umbella*. Local bioturbations are also observed. Facies are dominated by mudstones with ostracods and crinoids and with local coarser levels with fossils of mostly open origin, without algae (the few algae are strongly altered) indicating deposition in a quiet setting (below the FWWB), probably below the photic zone but sporadically affected by storms. In the biostromal belt (N3), biostromes are observed, with solitary rugose corals, branching stromatoporoids and tabulate corals but these biostromes are strongly dolomitized. The shallow belt (N4–N7) is made of subtidal to intertidal facies. Subtidal

facies are paleosiphonocladales packstones (facies N4 similar to C6, from CA) and microbial-algal packstone to boundstone with cyanophytes, porostromates, oncoids, *Sphaerocodium* and *Umbella*, with few ostracods, broken stromatoporoids and *Amphipora* (which can be the centre of oncoids) (facies N5). The intertidal zone presents wackestone or packstone with *Umbella* and mudstone with ostracods (N6, similar to C7) and laminar grainstone with peloids and clasts (N7, close to C8 but with coarser grains).

The Bovesse Formation has not been observed in continuous sections and is characterized by a lower acyclic part with shales (N1), mudstones with crinoids or gastropods (N2) and dolomitized biostromes (N3). The lower 40 m of the Huccorgne Formation corresponds to gastropods and crinoids mudstone to packstone (N2). Between 40 and 50 m there is a gap in the section and the upper part of the Huccorgne Formation is characterized by inner shallowing upward cycles (N4–N6). Two main units can be recognized, a lower biostromal unit, corresponding to the Bovesse Formation and the lower part of the Huccorgne Formation, and an upper lagoonal unit corresponding to the upper part of the Huccorgne Formation. These units are similar to the biostromal and lagoonal unit described in the CA. Although in this NA, a potential sequence boundary between the two units is not recognized because of the gap in the outcrop in the middle part of the Huccorgne Formation.

Interpretation of depositional model and facies evolution

All facies models (synthesis in Table 1) are characterized by strong facies similarity with minor differences between the different areas:

- Deep facies: shaley crinoidal material (S0, C1–C2 and N1–N2) or poorly diversified mud-rich mound facies (S2–S3). However, these facies are characterized by stromatactis and high mud content in the mounds from SA, micropackstones in the CA and gastropods and mud in the NA.
- 'Buildups' facies (S4–S5, C3–C5 and N3) dominated by reef-building organisms or boundstone with microbial structures. The dominant reef-builders are branching and bulbous stromatoporoids and microbes in the mounds from the SA; laminar, bulbous and branching stromatoporoids in the CA and tabulate corals and bulbous stromatoporoids in the NA (dolomitized biostromes).
- Shallow facies (S6–S8, C6–C9 and N4–N7) dominated by algae and peloids. These facies are similar in all the Areas; the main difference is the local occurrence of *Umbella* in the Central Lustin and NA and of oncoids in the NA.

In the mud mound succession (SA), each mud mound level is characterized by a lower phase with deep outer facies corresponding to transgressive and high stand conditions. After an important sequence boundary occurring in the middle of the mound, the upper mound is characterized by shallow mound inner facies in transgressive condition (Boulvain, 2007). The three mounds are divided by a sequence boundary. In the CA and NA, only one major sequence boundary was identified, dividing the sections, in a lower biostromal unit and an upper lagoonal unit (Fig. 2; Da Silva *et al.*, 2009a).

MAGNETIC SUSCEPTIBILITY

Ellwood *et al.* (2000) suggested that MS trends in sedimentary rocks depends on the lithogenic fraction (terrigenous contributions, para- and ferromagnetic contributions), which is related mainly to eustatism, or climatic changes. During sea-level lowstands, larger surface areas are subject to weathering and the detrital influxes to the world's oceans are higher (Davies *et al.*, 1977). Thus, theoretically, the highest MS magnitudes represent maximum sea-level lowstands and MS signal increases during a sea-level fall (Crick *et al.*, 1997). Lowest MS magnitude represent maximum sea-level highstands and decreasing MS occurs during rising sea level. MS has therefore been used as a proxy for sea-level variations (Devleeschouwer, 1999; Racki *et al.*, 2002; Hladil *et al.*, 2003; Da Silva & Boulvain, 2006). Atmospheric dust and eolian supplies were also identified as important mineral carriers (Hladil, 2002; Hladil *et al.*, 2006, 2010). During glaciations or increasing rainfalls, MS also increases.

Magnetic susceptibility in the SA

Magnetic susceptibility data are incomplete in the SA with some results presented on the La Boverie mound (Boulvain & Coen-Aubert, 2006). MS application allowed good correlations to be made between this mound from the Nord quarry and the surrounding mounds (distant of several tens of kilometres, Fig. 3a, b). In mound examples, MS is lower for the shallowest facies and decreases in regressive trends and is higher for the deepest facies and increases in transgressive trends (Fig. 3b). As described before, a sharp shallowing event is observed in all mound levels corresponding to the transition from deep mound to shallow mound (Boulvain, 2007). MS measurements have been made on this transition in the La Boverie mound (La Boverie quarry and Nord quarry, Fig. 3a, b) as well as in the Lion mound (Lompret section, see Da Silva *et al.*, 2009b) and in all these successions, shallowing is characterized by a sharp decrease of MS values.

Magnetic susceptibility in the CA

Complete MS curves are available on Neuville, Villers, Aywaille, Tailfer, Barse and Tillf sections (Fig. 5). If we consider the Tailfer section as a reference section, different trends (Fig. 4) are observed (complete description in

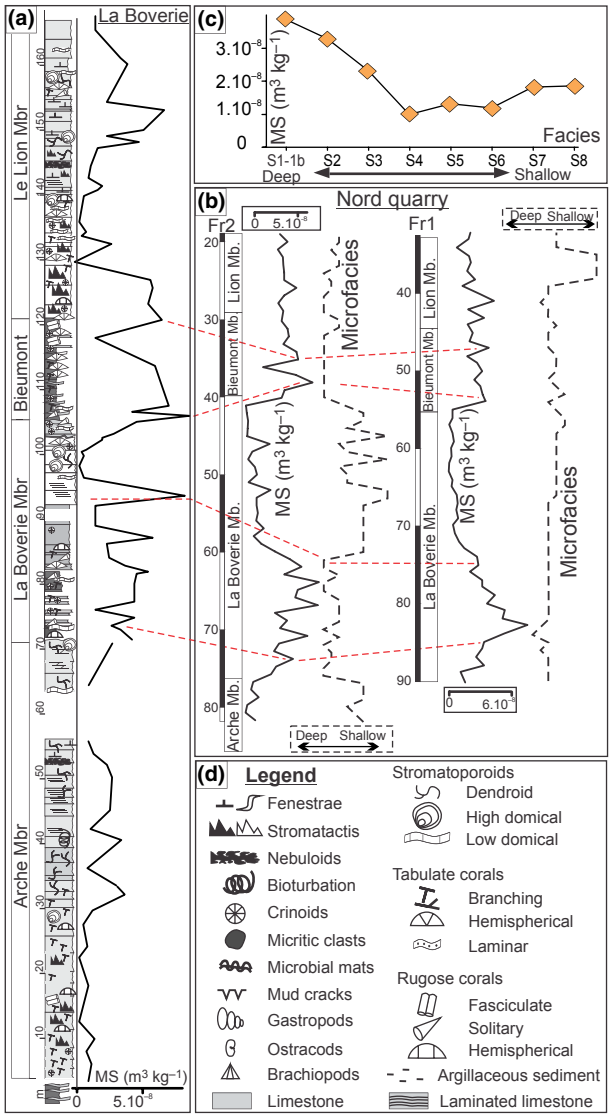

Fig. 3. Magnetic susceptibility evolution in the Southern Area. (a) Lithological column and magnetic susceptibility curve for La Boverie section after Boulvain *et al.* (2005); (b) formations, magnetic susceptibility, microfacies evolution from cores Fr1 and Fr2 in the Nord quarry (Boulvain & Coen-Aubert 2006); (c) mean magnetic susceptibility evolution from the Nord quarry cores with microfacies, after Da Silva *et al.* (2010); (d) legend for Figs 2, 4, 5 and 7.

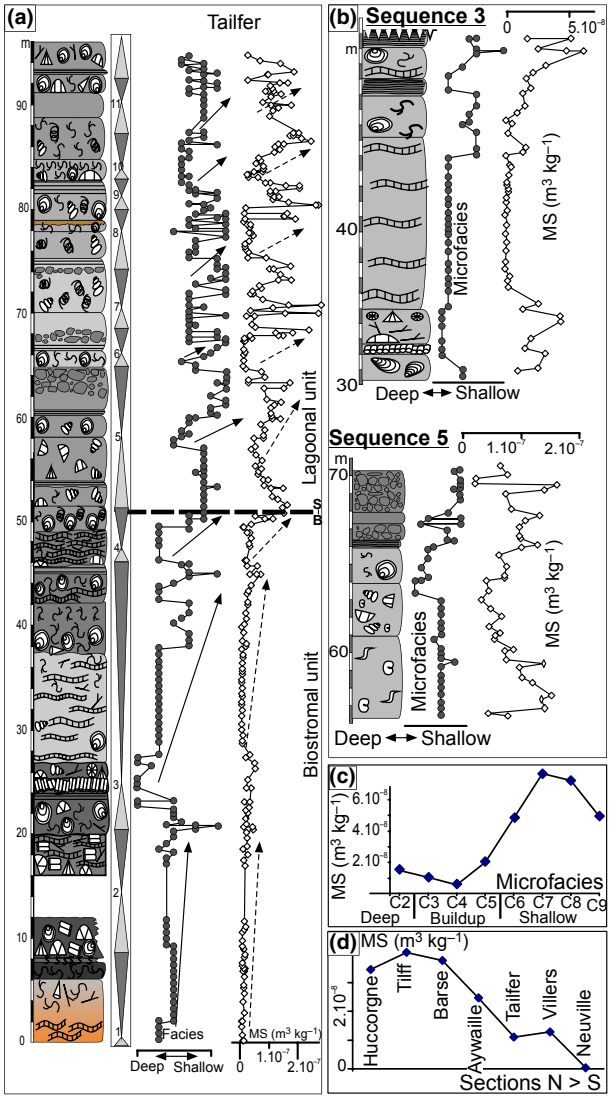

Fig. 4. Magnetic susceptibility evolution in the Central Area (a–c) and general trend on the whole platform (d). (a) Lithological column, microfacies evolution curve and magnetic susceptibility from Tailfer section (after Da Silva & Boulvain, 2002); (b) enlargement of Sequences 3 and 5 (after Da Silva & Boulvain, 2006) showing the strong link between magnetic susceptibility and microfacies; (c) evolution of mean magnetic susceptibility with microfacies (after Da Silva & Boulvain, 2006); (d) evolution of mean magnetic susceptibility for biostromal unit from the different studied sections. Legend is on Fig. 3d.

Da Silva & Boulvain, 2006): (1) subdivision of the curve in two distinct parts which corresponds to the biostromal unit (low MS values around 2×10^{-8} m³ kg^{-1}) and lagoonal unit (high mean values around 6.62×10^{-8} m³ kg^{-1}) (Fig. 4a); (2) Correlation of the cycles identified on the MS curve and the fourth-order sequences, each regressive trend corresponding to a MS peak on the MS evolution curve (Fig. 4b); (3) Strong relationship between MS and microfacies, with increasing mean MS related to proximality (Fig. 4c); (4) a comparison of the mean MS values of the biostromal unit of the different sections (Fig. 4d) shows that mean values are the highest in Tilff and Huccorgne (from NA) which are closest sections from the source and decrease with distance from source. The first trend (1) corresponding to the separation in a biostromal and lagoonal unit is clearly observed in all sections (Fig. 5). The cyclic (2) pattern is obvious in Villers, Aywaille and Barse but less clear in Neuville and Tilff. The similar pattern observed in most of the sections has been used to propose a correlation chart based on MS peaks (Fig. 5).

Magnetic susceptibility in the NA

The Huccorgne section is strongly fragmented and so fourth-order cyclicity is difficult to identify. However, as

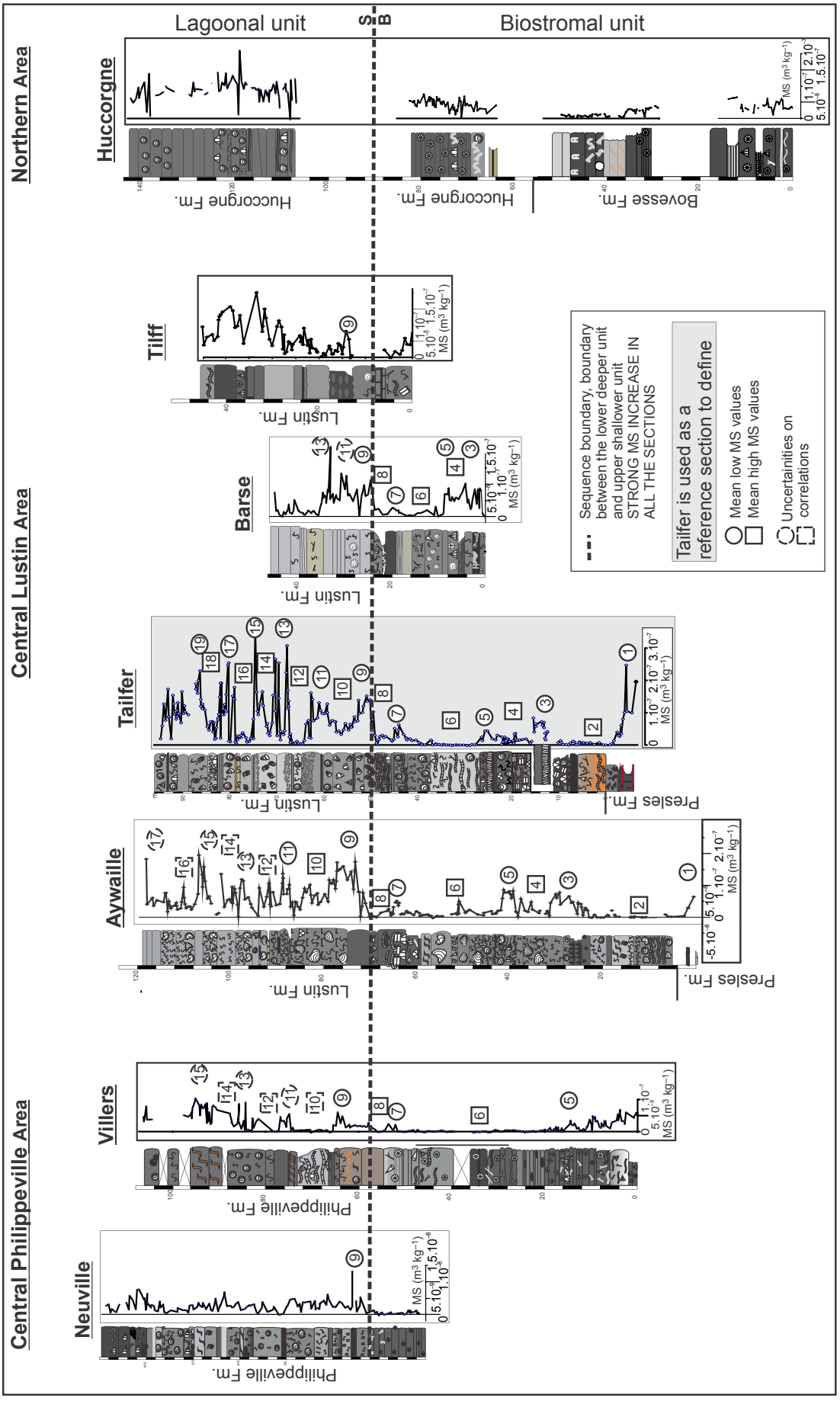

Fig. 5. Magnetic susceptibility evolution for the sections from Central and Northern Areas. The strong increase of MS at the boundary between biostromal and lagoonal unit is obvious in all sections. Legend is on Fig. 3d.

observed in the CA, the biostromal unit has mean lower MS values (3.4×10^{-8} m³ kg^{-1}) than the lagoonal unit (8.9×10^{-8} m³ kg^{-1}).

Interpretation of MS results

In the Central and Northern models, MS follows a classical proximal-distal trend related to the strong link between MS and lithogenic inputs (e.g. Ellwood *et al.*, 2000; Hladil, 2002; Da Silva *et al.*, 2009a) and offers good correlations between the sections. In the mound system (SA), good correlations in the same mound and between the mounds are observed (Boulvain & Coen-Aubert, 2006). However, there is an opposite correlation between MS and microfacies which could be explained by a stronger water agitation during deposition of the atoll crown and a protected environment inside the atoll crown. Furthermore, the occurrence of condensed levels and low carbonate productivity during lower mud mound deposition (facies S1–S3) could explain the higher MS values in the lower mound level (for complete explanation, see Da Silva *et al.*, 2009b). It is interesting to note that MS measurements from Quaternary mound systems (Porcupine mounds) have showed that these mud mounds are relatively independent systems, and that the susceptibility pattern from the mound itself cannot be recognized in the surrounding sediments (Foubert & Henriet, 2009).

CARBON ISOTOPES

Carbon isotopes in the SA

A carbon isotopic curve from the SA is proposed on micritic matrix from the upper part of the La Boverie

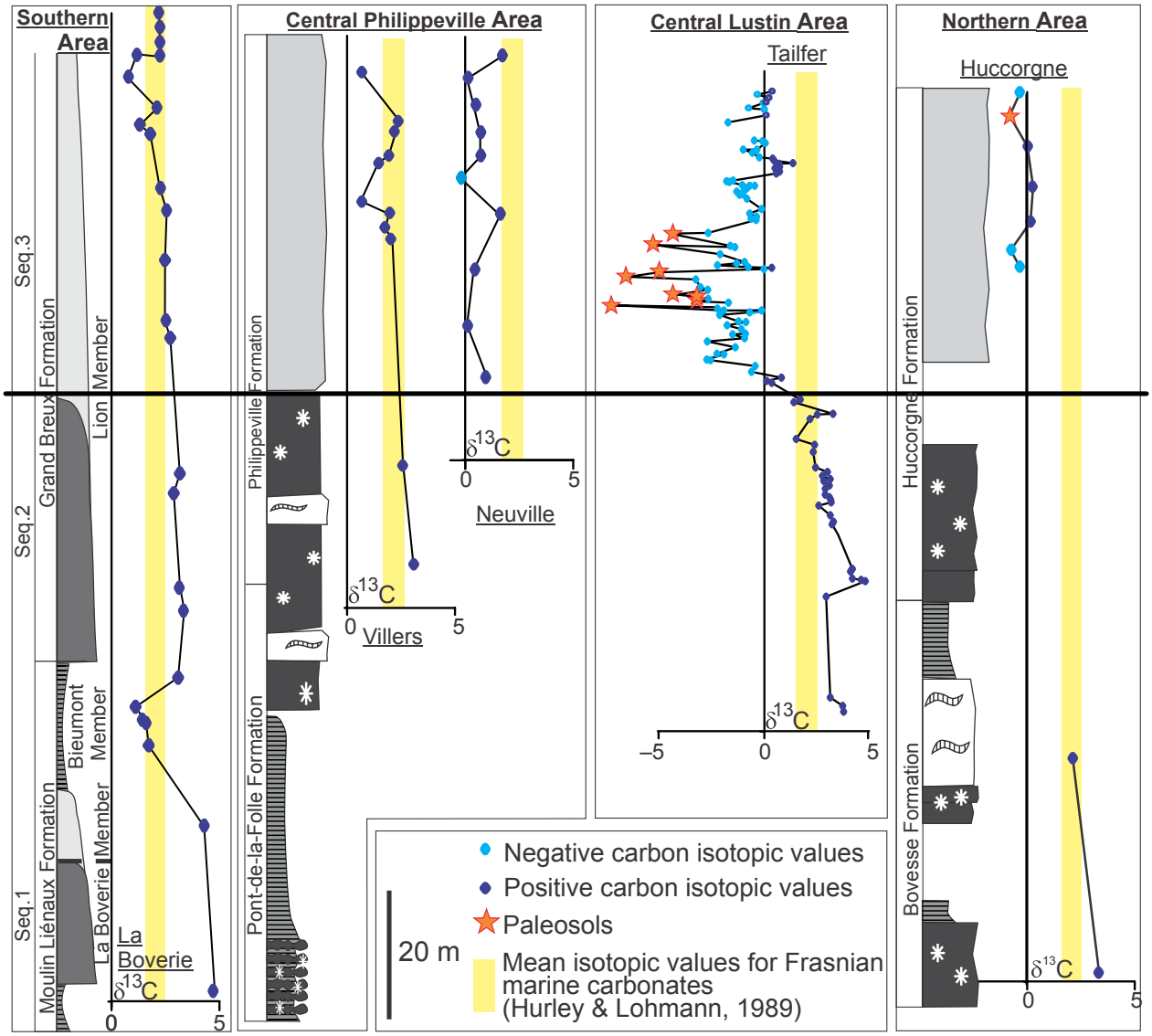

Fig. 6. Comparison of carbon isotopes trends for the different areas (data from Tailfer section were published in Da Silva & Boulvain, 2008). Sequences 1–2 present high values in all the sections. During Sequence 3, extremely low values are observed in the Central Lustin Area, low to intermediate values in the central Philippeville and Northern Areas and values close to the mean isotopic values for Frasnian marine carbonates in the Southern Area. Legend is on Fig. 2.

section (La Boverie, Bieumont and Lion members, Fig. 6). The argillaceous carbonates (S1) between the Arche and La Boverie mounds and deep mound (S2–S5) from the base of La Boverie mound have very high values, around 4.0‰. Then, the Bieumont Member (argillaceous carbonates, S1) presents low to high values (1.14–3.1‰) and the Lion Member shows values between 2.7‰ and 3.2‰ for the deep mound facies (lower part of the mound) and 1.4–2.5‰ for the lagoonal facies (upper part of the mound). These results are in agreement with the results published by Yans *et al.* (2007).

Carbon isotopes in the CL

A complete carbon isotopic curve for the Tailfer section is presented in Fig. 7 (Da Silva & Boulvain, 2008). Carbon isotope values of micritic matrix are highly variable (Figs 6 and 7) but the trend is clearly related to proximity with decreasing carbon isotope values with shallowing trends. Detailed results are presented in Da Silva & Boulvain (2008) and are synthesized herein: (1) the biostromal unit (Sequences 0–2) has mean $\delta^{13}C$ values constant around 3.0‰ and the lagoonal unit (Sequence 3) has a lower highly variable signature [mean values are negative (−1.2‰ $\delta^{13}C$), with some values being strongly negative (−7.5‰ $\delta^{13}C$) and the values are slightly increasing to the top of the lagoonal unit (0‰)]; (2) the isotopic ratios from the lagoonal unit of the Tailfer section seem to be related to the fourth-order sequences (Fig. 7a, b); (3) mean $\delta^{13}C$ values vs. microfacies shows more negative values of $\delta^{13}C$ from the deepest to the shallowest microfacies, with extreme negative values for the paleosols (Fig. 7c); (4) $\delta^{13}C$ data of the lagoonal unit are plotted against the intensity of exposure and carbon isotope signature becomes more negative with increasing intensity of subaerial exposure (Fig. 7d).

Carbon isotopes in the CPh

Further analyses are presented for the Neuville and Villers sections (Fig. 6). In Villers, the biostromal unit is characterized by values between 2‰ and 3‰ and the lagoonal unit, by values between 0.6‰ and 2.2‰, with a mean value of 1.62‰. The Neuville section, cutting only the lagoonal unit, presents values between −0.23‰ and 1.75‰, with a mean value of 0.8‰.

Carbon isotopes in the NA

The data obtained for the Huccorgne section are clearly in agreement with those observed for the Tailfer section, with high values (2.13‰ and 3.5‰) for the biostromal unit (Sequences 0–2) and negative or low values (0.45‰ and −0.8‰) for the lagoonal unit (Sequence 3). However, the low values, even for weakly pedogenetic facies, do not reach the negative values observed in Tailfer.

Interpretation of carbon isotopic trends

Detailed interpretations of the results from CA are published in Da Silva & Boulvain (2008). These interpretations are synthesized herein and compared with the new results to propose a model for the whole Belgian platform.

The signature of Frasnian seawater in Belgium is very different during deposition of Sequences 0–2, compared to Sequence 3. During deposition of Sequences 0–2 (biostromal unit), the carbon isotope values were constant and high (around 3.0‰; Fig. 7f) across the whole platform, indicating a homogeneous seawater composition (Fig. 7f), with only a negative peak above the Arche Member (Yans *et al.*, 2007). These positive values (and the negative peak) have also been observed in Moravia (Geršl & Hladil, 2004; Hladil *et al.*, 2009), China (Ma *et al.*, 2008), Canadian Rockies (Sliwinski *et al.*, 2010), Poland (Racki *et al.*, 2004; Pisarzowska *et al.*, 2006) and Nevada (Morrow *et al.*, 2009). This convergence of data confirms the reliability of the measurements and global oceanic connection between these high values.

The carbon mean isotopic data for the micritic matrix of Sequence 3 (lagoonal unit) are positive in La Boverie, Villers and Neuville, to negative in Tailfer and Huccorgne has an intermediate close to zero mean values. Furthermore, for the CL, C-isotopic values decrease for paleosols and to the top of fourth-order sequences (observation on Taifler section, the only section with detailed sampling). The evolution towards more negative carbon isotopic values has also been observed in literature, for the decreasing trend to the top of fourth-order regressive sequences (as in Algeo *et al.*, 1992; Joachimski, 1994; Hladil *et al.*, 2004, 2009) and transects from distal to proximal facies (Lloyd, 1964; Allan & Matthews, 1982). These low carbon isotope values could eventually be related to early meteoric diagenesis, or it could be that regionally Frasnian seawater became depleted in ^{13}C in some areas of the platform. The second hypothesis seems more likely, as a clear distal-proximal decreasing trend is observed (Fig. 7c–f). In the case of modern semi-restricted marine environments, the influence of the local carbon cycle on $\delta^{13}C$ can be substantial. Effectively, the shallow-water of Florida Bay and the Bahama Platform has a $\delta^{13}C$ value of 4.0‰ lower than the open ocean surface water (Lloyd, 1964; Patterson & Walter, 1994). These low values have been linked to the input of ^{12}C from remineralized organic carbon during the long residence time 'ageing' of the water on the platform (Patterson & Walter, 1994). This kind of lateral variation, with the lowest carbon isotope values in the shallowest part of the platform, has also been observed in Palaeozoic sediments (see e.g. Holmden *et al.*, 1998; Immenhauser *et al.*, 2002), and could explain the carbon isotopic values observed. All the trends obtained here correspond to a proximal-distal gradient in $\delta^{13}C$ values, with the lowest values being in the shallowest zones (Figs 6 and 7) and this was confirmed by the new data, from La Boverie,

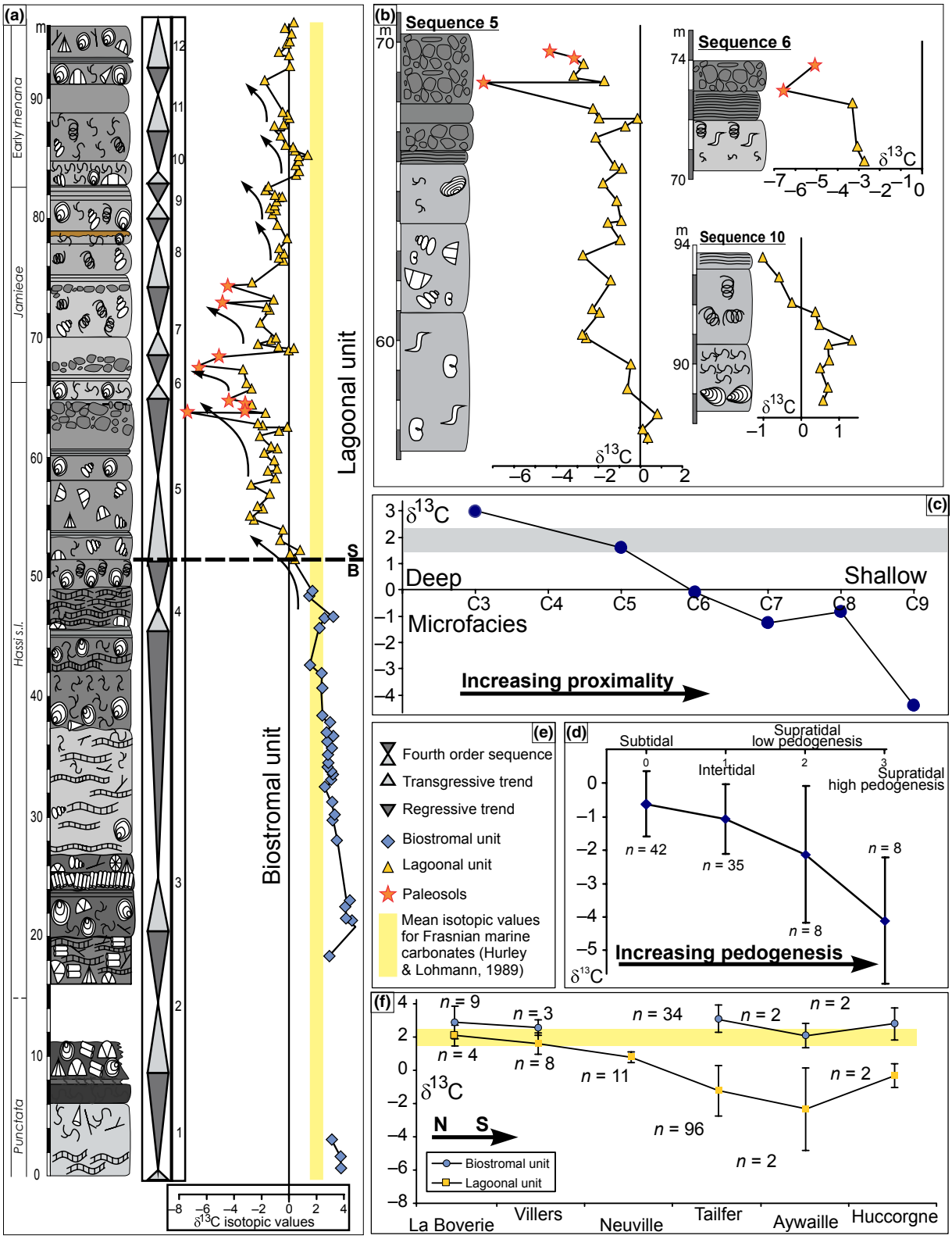

Fig. 7. Carbon isotopic evolution in the Central Area Tailfer section (a–d) and trends on the whole platform (f). (a) Tailfer section, with conodont zones (Gouwy & Bultynck, 2000) and carbon isotopic curve an units; (b) enlargement of shallowing upward sequences and carbon isotopic curve decreasing to the top and reaching strongly negative values for the paleosols (stars) and less negative values for sequences not affected by pedogenesis; (c) mean carbon isotopic evolution on a distal-proximal microfacies transect; (d) mean carbon isotopic values compared to the pedogenetic rate; (e) legend for sequences, and isotopic curves; (f) mean isotopic values for all sections during the biostromal and lagoonal units (n = number of samples). During the biostromal unit, mean values are high and constant and during the lagoonal unit, the values are decreasing on a distal-proximal trend. Legend for lithological column is on Fig. 3d. (a–d) are modified from Da Silva & Boulvain (2008).

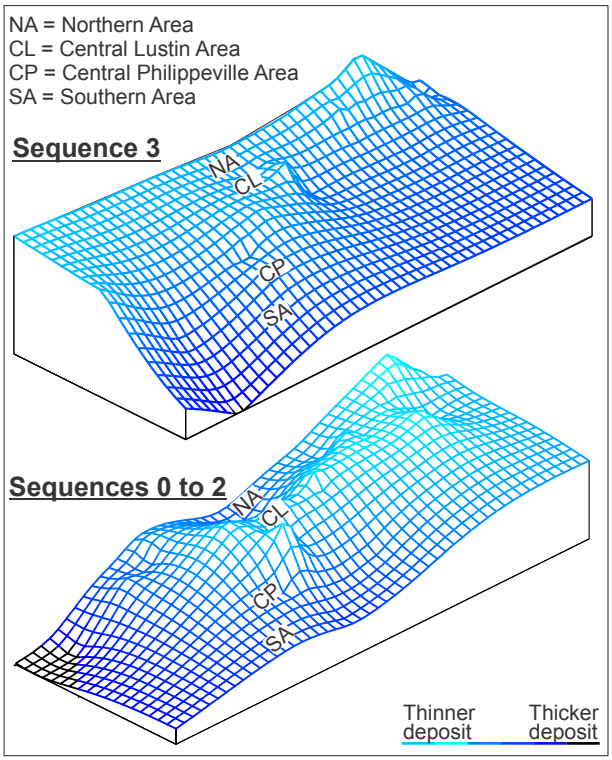

Fig. 8. Thickness distribution of Frasnian successions in Belgium. The graphs were overturned, so the less thick successions are corresponding to the 'shallowest' areas and the thickest successions to the 'deeper' areas. For definition of Sequences 0–3, see text chapter sedimentology and cyclicity of Southern Area and Fig. 2.

Villers, Huccorgne and Neuville. La Boverie having values close to published carbon isotope values for Devonian marine carbonate (e.g. Hurley & Lohmann, 1989; between 1.5‰ and 2.5‰). The uppermost few metres of the Lustin Formation (CA), are characterized by a transgression, with the reappearance of an open marine fauna including crinoids and brachiopods. The carbon isotope signatures increased with the transgression and, at the top of the Lustin Formation (Fig. 7), carbon isotope values are around zero, which corresponds probably to a reopening of the Belgian Frasnian sea and increasing water circulation [a rapid deepening will enhance water circulation and aged platform water will be mixed with open marine water masses, leading to a carbon isotope positive trend (Immenhauser *et al.*, 2002)].

CORRELATIONS AND THICKNESS DISTRIBUTION

A correlations chart (Fig. 2) has been constructed from two main sources: (1) MS results (Fig. 5) and (2) graphic correlations published by Gouwy & Bultynck (2000) and based on the presence of conodonts, brachiopods, corals, stromatoporoids and bentonite layers. The most important result of these correlations is that strata of the *punctata* conodont zone shows strong lateral variations in thickness from NA to SA. The *punctata* conodont Zone is about 110 m in the SA; around 60 m in the CPh, only 15 m in the CL and 50 m in the NA (Gouwy & Bultynck, 2000). So in the CL, *punctata* conodont Zone is very thin compared to the other Areas. In the 'Sedimentology, facies and cyclicity' section, the sedimentological evolution of the mounds was described, and the successive mound levels are all characterized by a sequence boundary dividing the three mounds in a lower deeper part and an upper shallower part. The two lowest mounds levels (Arche and La Boverie, Sequences 0–1), corresponding mostly to the *punctata* conodont Zone are very difficult to precisely correlate with the central model considering the thickness reduction in this area. However, the sequence boundary in the Lion mound (SA, sequence boundary 3 on Fig. 2) can be correlated with the sequence boundary in the CA and NA corresponding to the transition from the lower biostromal unit and upper lagoonal unit (see Figs 2 and 5; Boulvain *et al.*, 1994; Da Silva *et al.*, 2009b) and located in the middle of the *hassi* conodont Zone.

To provide thickness distribution graphs to improve understanding the geometry of the platform, thicknesses of stratigraphic intervals from different locations were collected in the field or from literature (a complete table of thickness and related references in Da Silva, 2004). Each outcrop was located on a grid (coordinates) and was associated with its thickness. A 3D graphic of thickness distribution was made using the programme Surfer® and the graphic obtained were overturned to represent the lowest thickness areas in relief and the higher thickness as deeper zones. Two 3D plots of thickness distribution are presented (Fig. 8), one corresponding to the Sequences 0–2, *punctata* to the middle part of *hassi* (Fig. 2) and the second corresponding to Sequence 3, *hassi* to base of Lower *rhenana* (Fig. 2). The SB3 boundary was chosen for two main reasons: (1) SB3 is the only boundary that can be traced through the SA, CA and NA; (2) SB3 corresponds to major changes of facies, MS and carbon isotopes and (3) SB3 corresponds to the boundary between the biostromal unit and the lagoonal unit and was recognized for a long time in the literature and lots of data are available on the thickness distribution of these two units.

Following these premises, sequences, correlations and thickness distribution are as follows:

- Sequences 0–1: Arche and lower part of the La Boverie Membre in the SA; corresponding to the major part of the Pont de la Folle Formation in the CPh; to very limited deposition in the CL and to most part of the Bovesse Formation in the NA (Fig. 2). Until now, we are not able to provide the lateral variations and location of SB1 considering the lack of continuous outcrop of the Pont de la Folle and Bovesse formations and the reduced thickness of this interval in the CL.

- Sequence 2: upper La Boverie, Bieumont and lower part of the Lion members (Fig. 2) in the SA, corresponds to the lower part of the Philippeville Formation (biostromal unit) and most of the biostromal unit of the Lustin Formation in the CA and to the biostromal unit of the Huccorgne Formation in the NA. For the same reason as mentioned below for SB1, we could not provide the lateral variations of SB2.

Thickness distribution of Sequences 0–2 presents strong relief, with a very shallow zone corresponding to the CL (lowest thickness in the northern part of the CA, corresponding to the southern border of the Namur Synclinorium). On both sides of this low subsidence zone, deeper zones (higher subsidence) are observed, corresponding to the SA, CPh and NA (Fig. 8). This difference of sediment thickness distribution between the different areas was probably even stronger considering differential compaction; facies from SA, CPh and NA (mostly deep outer deposits and shales) being more sensitive to compaction than the facies observed in the CL (pure limestones).

- Sequence 3: upper Lion Member in the SA, corresponding to the lagoonal unit of the Philippeville, Lustin (CA) and Huccorgne (NA) formations. Thickness distribution presents a 'classical' morphology, without strong evidence of synsedimentary block faulting (Fig. 8).

It is also interesting to note that Sequences 0 and 1 were deposited during a relatively short time (about 0.5 my for the two sequences), when Sequences 2 and 3 were deposited during a larger time (at least 0.7 Myr for Sequence 2 and at least 1 Myr for Sequence 3) (Gouwy & Bultynck, 2000; Kaufman, 2006). This difference in the duration of sequences also supports the scheme of a platform strongly affected by block faulting and synsedimentary tectonic control.

DISCUSSION – PLATFORM STRUCTURE AND SEA WATER CIRCULATION THROUGH TIME

The Frasnian is globally transgressive (Johnson *et al.*, 1985; Sandberg *et al.*, 2002) with superimposed regressive events. A synthesis of these main sea-level changes for Belgium is based on the mound succession and previously published results (Fig. 2; Boulvain, 2007; Da Silva *et al.*, 2010). A platform model and its evolution through time is presented on Fig. 9 and all the characteristics from the different Areas are summarized on Table 2.

During deposition of Sequences 0 and 1 (Figs 2 and 9c, most part of the *punctata* conodont Zone, only the upper part is missing), differences between the four paleogeographic Areas are maximal, with high subsidence in the SA and development of two mounds levels (at least 150 m thick) in an outer deep platform setting and lowest subsidence in the CL (about 10–15 m thick). The graph of thickness variation also shows that the CL corresponds to an east-west shallow-water ridge characterized by very low physical accommodation. The fault at the boundary between the SA and CPh has been described by Dumoulin *et al.* (1998) and Boulvain (2001) and is confirmed here. In the Lower Frasnian platform of the Canning Basin in Australia, the platform evolution is also strongly affected by syn-sedimentary faulting (George *et al.*, 2009). George *et al.* (2009) highlighted some important features related to the block faulting which are also observed in our case such as: (1) generation of differential subsidence which controlled major lateral and vertical facies distribution; (2) generation of topography filled with siliciclastic facies (in our case, the Pont de la Folle Formation and Ermitage Member); (3) promoting subaerial exposure of footwall high possibly in conjunction with sea-level falls (in our case, this is mostly during deposition of Sequence 3; and (4) control on major flooding and associated backstepping (e.g. a major backstepping event is observed between the Givetian and the Frasnian; Boulvain *et al.*, 2009).

During deposition of Sequences 0 and 1, in the SA, development of the Arche mound began under transgressive conditions, with deep mound facies. Then a marked sea-level drop (SB1, Fig. 2) led to local emersion of the mound (Sandberg *et al.*, 1992) and strong reworking and is followed by the next transgressive stage, with atoll and lagoonal deposits. Continued transgressive conditions and inability for carbonate production to keep up is indicated by the Arche mound being drowned and overlain by shales. Following this, the La Boverie mounds start growing within deep environments and just as for the Arche mound, a sea-level drop led to local emersion of the mound and reworking (SB2, Fig. 2) and is followed by the next transgressive stage, with lagoonal deposits (beginning of Sequence 2). The SB1 and SB2 were not observed in the CA and NA. This could be related to a thin stratigraphic development; and Sequence 0 and 1 and the SB were not recorded in relation with the active syn-sedimentary tectonic and to the shallow sea level at this time. Another reason to explain the nonobservation of SB1 and SB2 could be the poor outcrop quality (shaley and dolomitized, not continuous outcrops) and even if the SB were deposited, they are not well exposed on the field.

During deposition of Sequence 2 (Figs 2 and 9c, Lower *hassi* conodont Zone), observed sedimentological, faunal, geochemical and thickness features are similar than during deposition of Sequence 1. The platform structure did not change and they are still strong differences between the NA, CA and SA. In the SA, the lower Lion mound, developed in deepwater facies. In the CPh, deep outer crinoidal micropackstones (from the lower part of the Philippeville Formation) are deposited and the CL is dominated by biostromes. The NA also presents deep outer platform deposits but dominated by gastropods

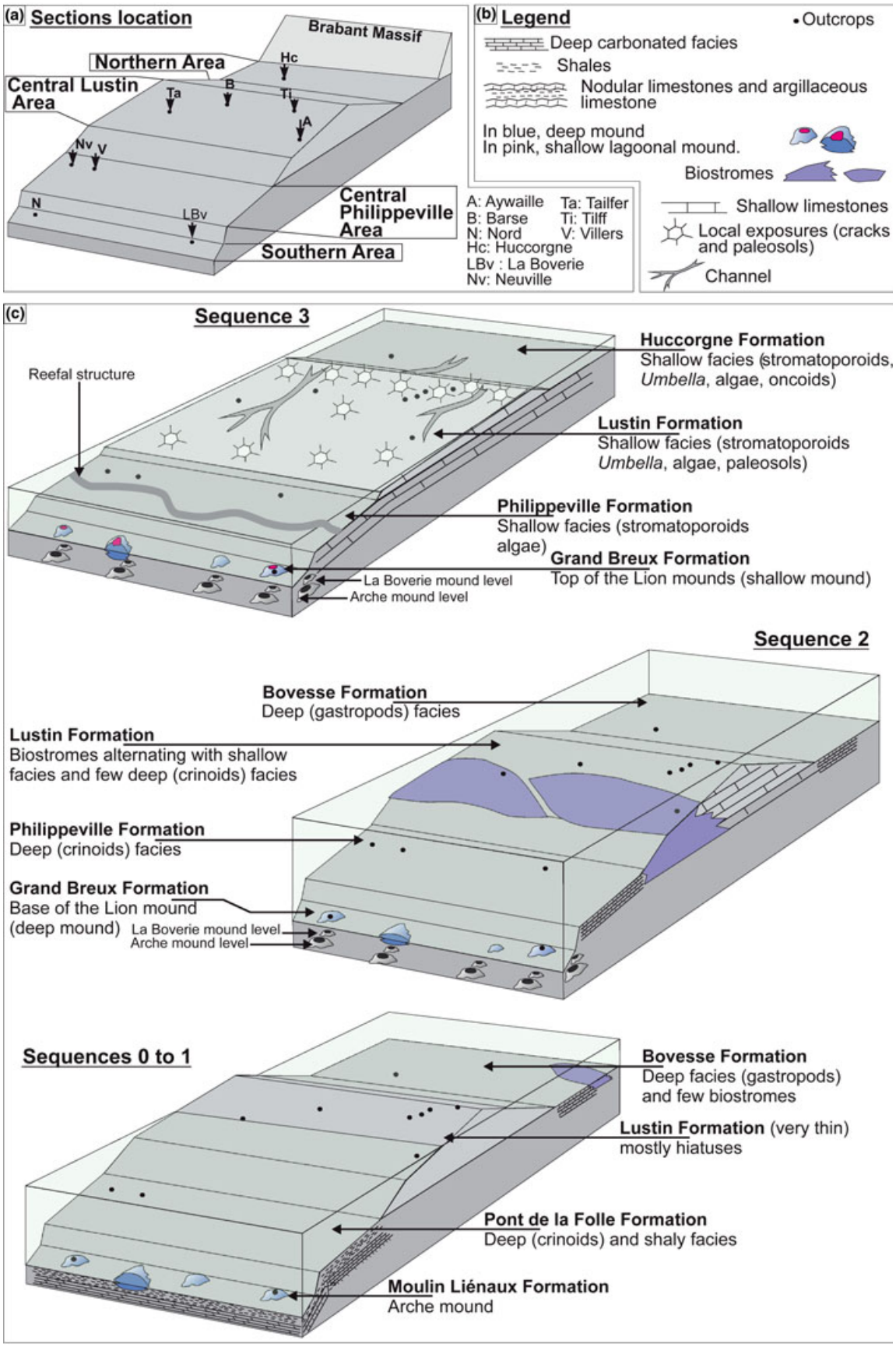

Fig. 9. Reconstruction of the Frasnian Belgian platform. (a) Model with blocks separated by syn-sedimentary faults with areas and location of the sections; (b) legend; (c) Frasnian platform in Belgium during Sequences 0–3 (see text chapter sedimentology and cyclicity of Southern Area and Fig. 2 for definition of Sequences).

Table 2. Main characteristics (main paleoenvironment, fauna, MS, carbon isotopes and thickness) for each model during Sequences 0–2 and Sequence 3

			Central Area		
	SEQ	Southern Area	Philippeville	Lustin	Northern Area
Palaeoenvironments	3	Atoll and lagoon, shallow mound	Shallow water subtidal to intertidal deposits	Shallow water subtidal to supratidal deposits	Shallow water subtidal to intertidal deposits
	0–2	Alternation deep and shallow mound	Deep and biostromal deposits	Biostromes with some shallow subtidal facies	Deep and biostromal deposits
Fauna	3	Stromatoporoids, algae microbialites, peloids	Stromatoporoids, peloids, algae	Stromatoporoids, peloids, algae, *Umbella*	Stromatoporoids, peloids, algae, oncoids, *Umbella*
	0–2	Stromatoporoids, corals, crinoids, stromatactis, algae microbialites, peloids	Crinoids, brachiopods, stromatoporoids	Crinoids, stromatoporoids, algae	Crinoids, gastropods
MS ($m^3\ kg^{-1}$)	3	2×10^{-8}	4.6×10^{-8}	$4.6–8.8 \times 10^{-8}$	8.9×10^{-8}
	0–2	2×10^{-8} Lower for shallow facies Higher for deep facies	1.2×10^{-8} Higher for shallow facies Lower for deep facies	$1.2–4 \times 10^{-8}$	3.5×10^{-8}
Carbon isotopes (‰)	3	+2	+2	−1 to −8	0 to −1
	0–2	+1 to +4	+3	+3 to +5	+3
Thickness	3	Gentle slope to the south			
	0–2	Strong relief – structuration in four main parts with different subsidence			

SEQ, sequence (see text chapter sedimentology and cyclicity of Southern Area and Fig. 2 for definition of sequences).

wackestone (high mud content), alternating with a few biostromes.

During the lower three sequences, carbon isotope values are high and similar not only in all Areas but also in other oceans. This close relationship between our values and worldwide trends is explained by open ocean conditions with good circulation. Furthermore, MS values are similar in all the Areas (Table 2; Fig. 5), corresponding to a good and homogeneous distribution of these inputs into the whole basin, also indicating good circulation. Lagoonal zones are not widely developed and biostromes are characterized by strong reworking (facies C4 floatstone with high domical stromatoporoids). These characteristics (good oceanic circulation, wide distribution of detritic inputs, limited development of lagoonal facies and marked reworking of biostromes) tend to point to an open ocean during the development of Sequences 0, 1 and 2. It is noteworthy that despite the existence of syn-sedimentary relief commonly associated with linear barrier reef complexes (Bosence, 2005) such structures seemed to be poorly developed or absent. This could probably be explained by the fact that the platform is still in an early stage, just developing on top of shales (Nismes and Presles formations).

Sequence boundary SB3 (Fig. 2) corresponds to a major event, associated with major paleogeographic changes (platform geometry and water circulation). After this event, the lagoonal palaeoenvironments developed everywhere on the CA and NA. Furthermore, thickness distribution presents a much more regular model with the disappearance of the east–west shallow-water ridge and the development of a platform with a more gentle slope. The CL and NA seem to be isolated from open sea as shown by the occurrence of new biotas such *Umbella* which are well known to develop in abnormal salinity zones (Mamet, 1970) and by the strongly negative carbon isotopic values (related to 'ageing', corresponding to the long residence time of the shallow water in this restricted ocean, Patterson & Walter, 1994). Furthermore, MS values show strong variations (Fig. 5), consistent with changes in local circulation and platform structure. In the NA, facies are similar than the CA (shallow subtidal to supratidal), but no paleosols are observed and isotopes are close to what is observed in CPh. So, the NA was likely deeper than the CL, indicating that block faulting is still slightly active.

So the Sequences 0, 1 and 2 were deposited in a faulted terrain (blocks) with open communication with the ocean and a poorly developed barrier reef; whereas Sequence 3 corresponds to a strongly restricted CA and NA (generalized lagoonal facies, *Umbella* and low $\delta^{13}C$) which point to a better developed reefal structure probably at the southern boundary of the CAs (Fig. 9c). In the SA (and in the south of the barrier reef), mud mounds still developed in a deep setting basin (Boussu-en-Fagne shale Member) and their growth, with development of sequence boundary 3 lead to the development of an atoll crown with shallow-water deposits.

CONCLUSIONS

It is difficult to reconstruct the Belgian Frasnian platform because of the overprinting by diagenesis and tectonic deformation. In this article, we have used a combination of techniques (facies, magnetic susceptibility (MS), stable isotopic variations and thickness distribution) to propose an integrated model (sea-level changes, water circulation, geometry, tectonics, detritic inputs, etc.) of the Belgian Frasnian platform.

Paleogeographic evolution of the platform involved two main phases separated by a major sequence boundary (karstic features, pendant cement, red staining, pedogenesis, clays):

- Sequences 0–2 – *punctata* to Lower *hassi*: the basin is strongly influenced by tectonics (block faulting), with a shallow-water ridge in the centre surrounded by deep outer platform deposits. The deepest zone developed in the south of the basin (SA), showing a succession of mud mound levels (two complete mounds and the base of a third one reaching about 200 m thick in total). During this interval, carbon isotopes and MS show little variation and are indicative of an open ocean and good water circulation, without well developed barrier reef.
- Sequence 3 – Upper *hassi* to Lower *rhenana*: the impact of block faulting is less significant and facies are more widely distributed across the platform. Furthermore, isotopes and MS as well as fauna are indicative of a very restricted platform, with restricted water circulation, probably resulting from better developed barrier reef.

ACKNOWLEDGEMENTS

A. C. Da Silva acknowledges the F.N.R.S. for a position of postdoctoral researcher. Special thanks to James Gardner (Royal Holloway, University of London, UK) for very helpful review and comments on an earlier version of this article. This article is part of the IGCP-580 project 'Application of magnetic susceptibility as a palaeoclimatic proxy on Palaeozoic sedimentary rocks and characterization of the magnetic signal' (UNESCO, IUGS). We would like to strongly acknowledge the reviewers (A. George, J. Hladil and P. Koenigshof) as well as the Editor I. Montanez for excellent reviewing work which strongly improved the article.

REFERENCES

Adams, R. & Vandenberghe, N. (1999) The Meuse section across the Condroz-Ardennes (Belgium) based on a predeformational sediment wedges. *Tectonophysics*, **309**, 179–195.

Algeo, J.T., Wilkinson, B.H. & Lohmann, K.C. (1992) Meteoric – burial diagenesis of Middle Pennsylvanian limestones

in the Orogrande Basin, New Mexico: water/rock interactions and basin geothermics. *J. Sed. Petrol.*, **62**, 652–670.

Allan, J.R. & Matthews, R.K. (1982) Isotope signatures associated with early meteoric diagenesis. *Sedimentology*, **29**, 797–817.

Bosence, D. (2005) A genetic classification of carbonate platforms based on their basinal and tectonic settings in the Cenozoic. *Sed. Geol.*, **175**, 49–72.

Boulvain, F. (2001) Facies architecture and diagenesis of Belgian Late Frasnian carbonate mounds. *Sed. Geol.*, **145**, 269–294.

Boulvain, F. (2007) Frasnian carbonate mounds from Belgium: sedimentology and palaeoceanography. In: *Palaeozoic Reefs and Bioaccumulations: Climatic and Evolutionary Controls* (Ed. by J.J. Alvaro, M. Aretz, F. Boulvain, A. Munnecke, D. Vachard & E. Vennin) *Geol. Soc. London, Spec. Publ.*, **275**, 125–142.

Boulvain, F. & Coen-Aubert, M. (1997) Le monticule Frasnien de la carrière du Nord à Frasnes (Belgique): sédimentologie, stratigraphie séquentielle et coraux. *Serv. Géol. Belgique Prof. Paper*, **285**, 47 p.

Boulvain, F. & Coen-Aubert, M. (2006) A fourth level of Frasnian carbonate mounds along the South side of the Dinant Synclinorium (Belgium). *IRSNB Bull.*, **76**, 31–51.

Boulvain, F., Coen-Aubert, M., Dumoulin, V. & Marion, J.-M. (1994) La Formation de Philippeville à Merlemont: contexte structural, comparaison avec le stratotype et paleoenvironnements. *Serv. Geol. Belgique Prof. Papers*, **269**, 29 p.

Boulvain, F., Bultynck, P., Coen, M., Coen-Aubert, M., Helsen, S., Lacroix, D., Laloux, M., Casier, J.G., Dejonghe, L., Dumoulin, V., Ghysel, P., Godefroid, J., Mouravieff, N., Sartenaer, P., Tourneur, F. & Vanguestaine, M. (1999) Les Formations du Frasnien de la Belgique. *Memoirs Geol. Surv. Belgium*, **44**, 125.

Boulvain, F., Cornet, P., Da Silva, A.C., Delaite, G., Demany, B., Humblet, M., Renard, M. & Coen-Aubert, M. (2004) Reconstructing atoll-like mounds from the Frasnian of Belgium. *Facies*, **50**, 313–326.

Boulvain, F., Demany, B. & Coen-Aubert, M. (2005) Frasnian carbonate buildups of southern Belgium: the Arche and Lion Members interpreted as atolls. *Geol. Belgica*, **8**, 69–89.

Chen, D., Tucker, M.E., Jiang, M. & Zhu, J. (2001) Long-distance correlation between tectonic-controlled, isolated carbonate platforms by cyclostratigraphy and sequence stratigraphy in the Devonian of South China. *Sedimentology*, **48**, 57–78.

Crick, R.E., Ellwood, B.B., El Hassani, A., Feist, R. & Hladil, J. (1997) Magnetosusceptibility Event and Cyclostratigraphy (MSEC) of the Eifelian – Givetian GSSP and associated boudary sequences in North Africa and Europe. *Episodes*, **20**, 167–175.

Da Silva, A.C. (2004) *Sédimentologie de la plate-forme carbonatée frasnienne belge*. PhD Thesis, Université de Liège, Liège, 253 pp, http://hdl.handle.net/2268/26132.

Da Silva, A.C. & Boulvain, F. (2004) From palaeosols to carbonate mounds: facies and environments of the Middle Frasnian platform in Belgium. *Geol. Quart.*, **48**, 253–265.

Da Silva, A.C. & Boulvain, F. (2006) Upper Devonian carbonate platform correlations and sea level variations recorded in magnetic susceptibility. *Palaeogeogr. Palaeoclimat. Palaeoecol.*, **240**, 373–388.

Da Silva, A.C. & Boulvain, F. (2008) Carbon isotope lateral variability in a Middle Frasnian carbonate platform (Belgium): significance of facies, diagenesis and sea-level history. *Palaeogeogr. Palaeoclimatol. Palaeoecol.*, **269**, 189–204.

Da Silva, A.C., Mabille, C. & Boulvain, F. (2009a) Influence of sedimentary setting on the use of magnetic susceptibility: examples from the Devonian of Belgium. *Sedimentology*, **56**, 1292–1306.

Da Silva, A.C., Potma, K., Weissenberger, J.A.W., Whalen, M.T., Mabille, C. & Boulvain, F. (2009b) Magnetic susceptibility evolution and sedimentary environments on carbonate platform sediments and atolls, comparison of the Frasnian from Belgium and from Alberta. *Sediment. Geol.*, **214**, 3–18.

Da Silva, A.C., Yans, J. & Boulvain, F. (2010) Early-Middle Frasnian (Early Late Devonian) sedimentology and magnetic susceptibility of the Ardennes area (Belgium): identification of severe and rapid sea level fluctuations. In: *Magnetic Susceptibility, Correlations and Palaeozoic Environments* (Ed. by A.C. Da Silva & F. Boulvain) *Geol. Belgica*, **13-4**, 319–332.

Davies, T.A., Hay, W.W., Southam, J.R. & Worsley, T.R. (1977) Estimates of Cenozoic oceanic sedimentation rates. *Science*, **197**, 53–55.

Devleeschouwer, X. (1999) *La transition Frasnien-Famennien (Dévonien Supérieur) en Europe: sédimentologie, stratigraphie séquentielle et susceptibilite magnétique*. Thèse inédite Doctorat en Sciences présentée à l'Université Libre de Bruxelles, Bruxelles, 411 pp.

d'Omalius d'Halloy, J.G.J. (1862) *Abrégé de Géoologie*. 7ème édn, Schnee, Leiber, Bruxelles, Leipzig, Paris, 626 pp.

Dumoulin, V., Marion, J.-M., Boulvain, F., Coen-Aubert, M. & Coen, M. (1998) Nouvelles données lithostratigraphiques sur le Frasnien de l'Anticlinorium de Philippeville. *Ann. Soc. Géol. Du Nord*, **6**, 79–85.

Ellwood, B.B., Crick, R.E., El Hassani, A., Benoist, S.L. & Young, R.H. (2000) Magnetosusceptibility event and cyclostratigraphy method applied to marine rocks: detrital input versus carbonate productivity. *Geology*, **28**, 1135–1138.

Fielitz, W. (1992) Variscan transpressive inversion in the northwestern central Rheno-hercynian belt of Western Germany. *J. Struct. Geol.*, **14** (5), 547–563.

Fielitz, W. (1997) Inversion tectonics and diastathermal metamorphism in the Serpont Massif area of the Variscan Ardenne (Belgium). *Aardkd. Meded.*, **8**, 79–82.

Flügel, E. (2004) *Microfacies of Carbonate Rocks. Analysis, Interpretation and Application*. Springer-Verlag, Berlin, Heidelberg, New York, 976 pp.

Floyd, P.A. (1982) Chemical variation in Hercynian basalts relative to plate tectonics. *J. Geol. Soc.*, **139**, 505–520.

Foubert, A. & Henriet, J. (2009) *Nature and Significance of the Recent Carbonate Mound Record – the Mound Challenger Code*. Springer, Berlin Heidelberg, 298 pp.

Franke, W. (2000) The mid-European segment of the Variscides: tectonostratigraphic units, terrane boundaries and plate tectonic evolution. In: *Orogenic Processes: Quantification and Modelling in the Variscan Belt* (Ed. by W. Franke, V. Haak, O. Oncken & D. Tanner) *Geol. Soc. London, Spec. Publ.*, **179**, 35–61.

George, A.D., Playford, P.E., Powell, C.M. & Tornatora, P.M. (1997) Lithofacies and sequence development on an Upper Devonian mixed carbonate-siliciclastic fore-reef slope, Canning Basin, Western Australia. *Sedimentology*, **44**, 843–867.

George, A.D., Chow, N. & Trinajstic, K.M. (2009) Syndepositional fault control on Lower Frasnian platform evolution,

Lennard Shelf, Canning Basin, Australia. *Geology*, **37**, 331–334.

Geršl, M. & Hladil, J. (2004) Gamma-Ray and magnetic susceptibility correlation across a Frasnian carbonate platform and the search for "*punctata*" equivalents in stromatoporoid-coral limestone facies of Moravia. *Geol. Quart.*, **48**, 283–292.

Gouwy, S. & Bultynck, P. (2000) Graphic correlation of Frasnian sections (Upper Devonian) in the Ardennes, Belgium. *Bull. IRSNB*, **70**, 25–52.

Hardie, L.A. (1977) *Sedimentation on the Modern Carbonate Tidal Flats of Northwest Andros Island, Bahamas*. The J. Hopkins University Press, Baltimore & London, 202 pp.

Hladil, J. (2002) Geophysical records of dispersed weathering products on the Frasnian carbonate platform and early Famennian ramps in Moravia, Czech Republic: proxies for eustasy and palaeoclimate. *Palaeogeogr. Palaeoclimatol. Palaeoecol.*, **181**, 213–250.

Hladil, J., Bosak, P., Slavik, L., Carew, J.L., Mylroie, J.E. & Gersl, M. (2003) Early diagenetic origin and persistence of gamma-ray and magnetosusceptibility patterns in platform carbonates: comparison of Devonian and Quaternary sections. *Phys. Chem. Earth*, **28**, 719–727.

Hladil, J., Carew, J.L., Mylroie, J.E., Pruner, P., Kohout, T., Jell, J.S., Lacka, B. & Langrova, A. (2004) Anomalous magnetic susceptibility values and traces of subsurface microbial activity in carbonate banks on San Salvador Island, Bahamas. *Facies*, **50**, 161–182.

Hladil, J., Cejchan, P., Babek, O., Koptikova, L., Navratil, T. & Kubinova, P. (2010) Dust – a geology-orientated attempt to reappraise the natural components, amounts, inputs to sediment, and importance for correlation purposes. In: *Magnetic Susceptibility, Correlations and Palaeozoic Environments* (Ed. by A.C. Da Silva & F. Boulvain) *Geol. Belgica*, **13–4**, 367–384.

Hladil, J., Gersl, M., Strnad, L., Frana, J., Langrova, A. & Spisiak, J. (2006) Stratigraphic variations of complex impurities in platform limestones and possible significance of atmospheric dust: a study emphasis on gamma-ray spectrometry and magnetic susceptibility outcrop logging (Eifelian-Frasnian, Moravia, Czech Republic). *Int. J. Earth Sci.*, **95**, 703–723.

Hladil, J., Koptikova, L., Galle, A., Sedlacek, V., Pruner, P., Schnabl, P., Langrova, A., Babek, O., Frana, J., Hladikova, J., Otava, J. & Gersl, M. (2009) Early Middle Frasnian platform reef strata in the Moravian Karst interpreted as recording the atmospheric dust changes: the key to understanding perturbations in the punctata conodont Zone. *Bull. Geosci.*, **84**, 75–106.

Holmden, C., Creaser, R.A., Muehlbachs, K., Leslie, S.A. & Bergeström, S.M. (1998) Isotopic evidence for geochemical decoupling between ancient epeiric seas and bordering oceans: implications for secular curves. *Geology*, **26**, 567–570.

Hurley, N.F. & Lohmann, K.C. (1989) Diagenesis of Devonian reefal carbonates in the Oscar Range, Canning Basin, Western Australia. *J. Sed. Petrol.*, **59**, 127–146.

Immenhauser, A., Kenter, J.A.M., Ganssen, G., Bahamonde, J.R., Van Vliet, A. & S, M.H. (2002) Origin and significance of isotope shifts in Pennsylvanian carbonates (Asturias, NW Spain). *J. Sed. Res.*, **72**, 82–94.

Joachimski, M. (1994) Subaerial exposure and deposition of shallowing upward sequences: evidence from stable isotopes of Purbeckian peritidal carbonates (basal Cretaceous), Swiss and French Jura Mountains. *Sedimentology*, **41**, 805–824.

Johnson, J.G., Klapper, G. & Sandberg, C.A. (1985) Devonian eustatic fluctuations in Euramerica. *Geol. Soc. Am. Bull.*, **96**, 567–587.

Kasimi, R. & Preat, A. (1996) Eifelian-Givetian siliciclastic carbonate ramp systems, Belgium and France. Second part: cyclostratigraphy and paleostructuration. *Bull. Centres Rech. Explor.-Prod. Elf Aquitaine*, **20**, 61–90.

Lacquement, F. & Meilliez, F. (2006) Mise en evidence à l'affleurement de failles synsédimentaires majeures: exemple de la Faille de Vireux. *Géol. France*, **1–2**, 65–69.

Lloyd, M.R. (1964) Variations in the oxygen and the carbon isotope ratios of Florida bay molluscs and their environmental significance. *J. Geol.*, **72**, 84–111.

Ma, X.-P., Wang, C.-Y., Racki, G. & Racka, M. (2008) Facies and geochemistry across the Early-Middle Frasnian Transition (Late Devonian) on South China carbonate shelf: comparison with the Polish reference succession. *Palaeogeogr. Palaeoclimatol. Palaeoecol.*, **269**, 130–151.

MacNeil, A.J. & Jones, B. (2006) Sequence stratigraphy of a Late Devonian ramp-situated reef system in the Western Canada sedimentary basin: dynamic responses to sea-level change and regressive reef development. *Sedimentology*, **53**, 321–359.

Mamet, B.L. (1970) Sur les *Umbellaceae*. *Can. J. Earth Sci.*, **7**, 1164–1171.

Meilliez, F. & Mansy, J.L. (1990) Déformation pelliculaire différenciée dans une série lithologique hétérogène: Le Dévono-Carbonifère de l'Ardenne. *Bull. Soc. Géol. France*, **8**, 177–188.

Méndez-Bedia, I., Soto, F.M. & Fernández-Martínez, E. (1994) Devonian reef types in the Cantabrian Mountains (NW Spain) and their faunal composition. *Cour. Forsch. Senckenberg*, **172**, 161–183.

Morrow, J.R., Sandberg, C.A., Malkowski, K. & Joachimski, M.M. (2009) Carbon isotope chemostratigraphy and precise dating of Middle Frasnian (Lower Upper Devonian) Alamo Breccia, Nevada, USA. *Palaeogeogr. Palaeoclimatol. Palaeoecol.*, **282**, 105–118.

Oncken, O., Von Winterfeld, C.H. & Dittmar, U. (1999) Accretion of a rifted passive margin: The Late Paleozoic Rhenohercynian fold and thrust belt (Middle European Variscides). *Tectonics*, **18**, 75–91.

Paproth, E., Dreesen, R. & Thorez, J. (1986) Famennian paleogeography and event stratigraphy of northwestern Europe. *Ann. Soc Géol. Belg.*, **109**, 175–186.

Patterson, W.P. & Walter, L.M. (1994) Depletion of ^{13}C in seawater ECO_2 on modern carbonate platforms: significance for the carbon isotopic record of carbonates. *Geology*, **22**, 885–888.

Pisarzowska, A., Sobstel, M. & Racki, G. (2006) Conodont-based event stratigraphy of the Early-Middle Frasnian transition on the South Polish carbonate shelf. In: *Biotic Aspects of the Early-Middle Frasnian Eventful Transition* (Ed. by A. Balinski, E. Olempska & G. Racki) *Acta Palaeontol. Polonica*, **51**, 606–608.

Pohler, S.M.L. (1998) Devonian carbonate buildup facies in an intra-oceanic island arc (Tamworth Belt, New South-Wales, Australia). *Facies*, **39**, 1–34.

Racki, G., Racka, M., Matyja, H. & Devleeschouwer, X. (2002) The Frasnian/Famennian boundary interval in the South Polish-Moravian shelf basins: integrated event-stratigraphical approach. *Palaeogeogr. Palaeoclimat. Palaeoecol.*, **181**, 251–297.

Racki, G., Pietchota, A., Bond, D. & Wignall, B. (2004) Geochemical and ecological aspects of Lower Frasnian pyrite-ammonoïd level at Kostomloty (Holy Cross Mountains, Poland). *Geol. Quart.*, **48**, 267–282.

Salamon, M. & Königshof, P. (2010) Middle Devonian olistostromes in the Rheno-Hercynian zone (Rheinisches Schiefergebirge)—an indication of back arc rifting on the southern shelf of Laurussia. *Gondwana Res.*, **17**, 281–291.

Sandberg, C.A., Ziegler, A.M., Dreesen, R. & Butler, J.L. (1992) Conodont biochronology, biofacies, taxonomy and event stratigraphy around Middle Frasnian Lion mudmound (F2h), Frasnes, Belgium. *Cour. Forsch. Senckenberg*, **150**, 1–87.

Sandberg, C.A., Morrow, J.R. & Ziegler, W. (2002) Late Devonian sea-level changes, catastrophic events, and mass extinctions. In: *Catastrophic Events and Mass Extinctions: Impacts and Beyond* (Ed. by C. Koeberl & K.G. MacLeod) *Geol. Soc. Am. Spec. Paper*, **356**, 473–487.

Sliwinski, M.G., Whalen, M.T. & Day, J. (2010) Trace element variations in the Middle Frasnian *punctata* Zone (Late Devonian) in the Western Canada Sedimentary Basin – changes in oceanic bioproductivity and paleoredox spurred by a pulse of terrestrial afforestation? In: *Magnetic Susceptibility, Correlations and Palaeozoic Environments* (Ed. by A.C. Da Silva & F. Boulvain) *Geol. Belgica*, **13–4**, 459–482.

Strasser, A. & Hillgärtner, H. (1998) High-frequency sea-level fluctuations recorded on a shallow carbonate platform (Berriasian and Lower Valanginian of Mount Salève, French Jura). *Eclogae Geol. Helveticae*, **91**, 375–390.

Tsien, H.H. (1984) Récifs du Dévonien des Ardennes – paléoécologie et structure. In: *Géologie et Paléoécologie des Récifs* (Ed. by J. Geister & G. Herb) *Inst. Géol. Univ. Berne*, **7**, 7.1–7.30.

Vanbrabant, Y., Braun, J. & Jongmans, D. (2002) Models of passive margin inversion: implications for the Rhenohercynian fold-and-thrust belt, Belgium and Germany. *Earth Planet. Sci. Lett.*, **202**, 15–29.

Von Winterfeld, C.H. (1994) *Variszische Deckentektonik Und Devonische Beckengeometrie Des Nordeifel – Ein Quantitative Model. Profilbilanzierung Und Strain-Analyse Im Linksrheinischen Schiefergebirge*. Geologischen Institut der RWTH, Aachen, 319 pp.

Whalen, M.T., Eberli, G.P., Van Buchem, F.S.P. & Mountjoy, E.W. (2000) Facies models and architecture of Upper Devonian carbonate platforms (Miette an Ancient Wall), Alberta, Canada. In: *Genetic Stratigraphy on the Exploration and the Production Scales. Case Studies From the Pennsylvanian of the Paradox Basin and the Upper Devonian of Alberta* (Ed. by P.W. Homewood & G.P. Eberli) *Bull. Centres Rech. Explor.-Prod. Elf-Aquitaine, Mémoire*, **24**, 139–178.

Yans, J., Corfield, R.M., Racki, G. & Préat, A. (2007) Evidence for perturbation of the carbon cycle in the Middle Frasnian *Punctata* conodont Zone (Late Devonian). *Geol. Mag.*, **144**, 263–277.

Manuscript received 26 August 2010; In revised form 31 August 2011; Manuscript accepted 3 September 2011.